Transactions of the Korean Nuclear Society Spring Meeting
Jeju, Korea, May 9-10, 2024

Effect of Coating Material and Oxidation Model on the Fuel Performance Of Accident-Tolerant Fuel (ATF) with Multi-layered Cladding

Jiwon Mun, Hyeong-Jin Kim, Ho Jin Ryu *
Department of Nuclear & Quantum Engineering, Korea Advanced Institute of Science and Technology, 291 Daehakro, Yuseong, 34141, Republic of Korea
**Corresponding author: hojinryu@kaist.ac.kr*

1. Introduction

Since the Fukushima accident in 2011, accident-tolerant fuel (ATF) cladding has been actively developed to address the characteristics of zirconium alloys, which oxidize at high temperatures, generating heat by exothermic oxidation reaction and H_2 gas. A long-term solution is to replace zirconium-based alloys with new alloys such as iron-chromium-aluminium (FeCrAl) alloy, but a short-term solution is to apply an oxidation-resistant coating such as chromium (Cr) to the waterside, which has recently been actively researched. However, in the event of a burst or ballooning accident, the external coating cannot protect against internal oxidation, so the need for an internal coating is becoming increasingly important and has been the subject of some research [1]. Therefore, it is necessary to understand the thermo-mechanical performance of ATF cladding with such simultaneous inner and outer coatings.

Especially, with the recent need for load following operation in nuclear power plants to improve their economics, it is important to analyze the effect of the inner and outer coating on the frequent pellet-cladding interaction (PCI) that occurs during repeated power rise and fall [2].

In this study, a previously developed finite element analysis (FEA) system that reflects almost all multiphysics behavior of fuel rods was modified by adding various oxidation models. Through the modified finite element analysis system, multiphysics analysis of multiple-layered cladding especially focusing on the oxidation behavior was performed.

2. Methods and Results

2.1 Simulation conditions

In the present work, the improvement of the FEA system presented in the previous work, which is based on the ABAQUS^{TM} framework, was performed by adding additional oxidation models [3]. Detailed applied material correlation models and calculation conditions are mentioned in previous studies. The schematic of the multi-layered cladding used in this study is shown in Fig. 1. The calculations were performed considering the bare Zr-4 cladding case as shown in Fig. 1 (a) and the inner and outer coating case as shown in Fig. 1 (b). For coating materials, Cr and FeCrAl alloy were chosen. [4,5]. The maximum power is set to 35 kW/m, assuming a load-following scenario of 100 - 50 -100. The total operating period was 3 years, and the end-of-life (EOL) discharged burnup was calculated to be approximately 61 GWd/tU.

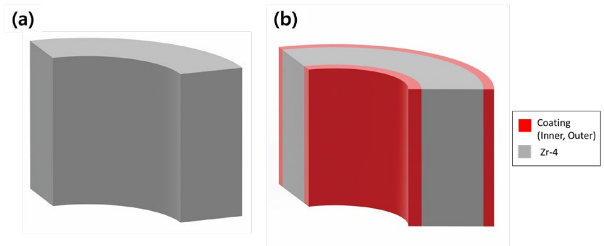

Fig. 1. Schematic of the (a) Bare Zr-4 cladding and (b) multi-layered cladding

The CAX4T element (4-node axisymmetric thermally coupled quadrilateral, bilinear displacement, bilinear displacement, and temperature) is chosen for the meshing scheme and the element type. The radial mesh of the cladding coating layer was set to 5. Axial direction symmetry boundary conditions and pressure boundaries were applied.

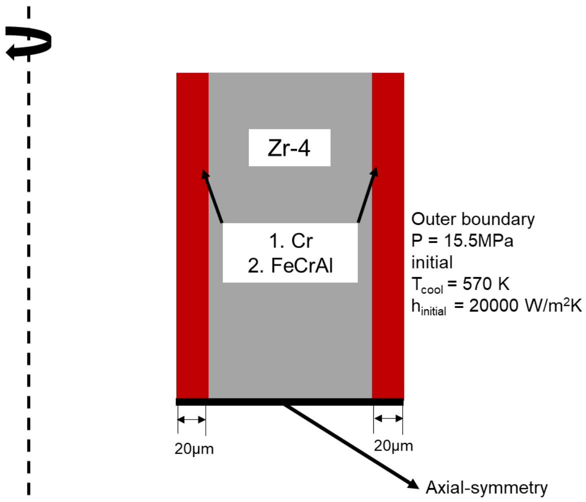

Fig. 2. Schematic of the initial boundary condition for cladding

2.2 Oxidation behavior model of the ATF cladding

In the evaluation of oxidation for the bare zirconium scenario, the well-known two-stage oxidation model was employed [6]. Initially, a cubic rate law governed the process up to a critical thickness of 2.0 μm as Eq.(2.1). Beyond this threshold, a linear rate law dependent on flux was utilized as Eq.(2.2). Furthermore, consistent with methodologies implemented in FRAPCON, the model anticipates the spallation of the zirconia oxide layer for thicknesses exceeding 150 μm. For FeCrAl case, the parabolic rate constant of Kanthal APMT alloy determined by Pint et al. was utilized to calculate mass gain by oxidation as Eq.(2.3) [7]. Also, oxide thickness was obtained by applying a conversion factor of 5.35 μm (cm^2/mg) as suggested by Jönsson et al [8]. In the case of Cr coatings, similar to FeCrAl coating, it has been experimentally reported that negligible mass gain occurs in normal operation, and Wagih et al. suggested using a conservative value for the mass gain of Zr divided by 15, which is the same methodology applied in this study [9].

<Zr-4 [6] >
Two–stage oxidation model

- Pre-transition

$$\frac{d(t_{oxide}{}^{3})}{dt} = C_1 \exp(\frac{-Q_1}{RT_1}) \ for \ t_{oxide} < t_{trans} \quad (2.1)$$

- Post-transition

$$\frac{dt_{oxide}}{dt} = C_2 \exp(\frac{-Q_2}{RT_1}) \ for \ t_{oxide} > t_{trans} \quad (2.2)$$

$t_{trans} = 2 \ \mu m$

$MAX(t_{oxide}) = 150 \ \mu m$ (assumption of oxide spallation over the thickness of 150 μm)

t_{oxide} : oxide thickness

<FeCrAl [7]>

$$k_p = k_o \exp(\frac{-Q_3}{T_1}), \ w_g = k_p{}^{1/2} t^{1/2} \quad (2.3)$$

w_g *: weight gain,*

As the oxide layer grows, the metal and oxide interface temperatures are updated automatically within the system as Eq.(2.4), and the oxide thermal conductivity used for each material is listed in the table below. In addition, the heat transfer coefficient has also been updated as the oxide has grown as Eq.(2.5).

$$T_{\text{interface}} = T_{cool} + \frac{q"}{k_{oxide}} t_{oxide} \quad (2.4)$$

$T_{\text{interface}}$: metal-oxide interface temperature

k_{oxide} : oxide thermal conductivity

$$h_{eff} = \frac{1}{\frac{1}{h_{initial}} + \frac{t_{oxide}}{k_{oxide}}} \quad (2.5)$$

h_{eff} : effective heat transfer coefficient considering oxide thickness

Table I: Oxide thermal conductivity parameters

k_{oxide}	*Design Value*
Zr-4, k_{ZrO2}	2.01
FeCrAl, k_{Al2O3}	30.0
Cr, k_{Cr2O3}	5.17

2.3 Calculation results

The fuel centerline temperature was calculated to be approximately 2000 K at 100% power level and 1200 K at 50% power level as shown in Fig. 3. The oxidation results are shown in Fig.4. As shown in Fig. 4, for the zr case, it was calculated that the transition thickness of 2 μm is reached at a burn-up of about 7 GWd/tU and then increases more steeply. In the current calculation, the maximum power is calculated at a relatively high power condition of 35 kW/m, so the spallation limit of 150 μm is quickly reached and then the maximum thickness is calculated to be maintained thereafter. In contrast, Cr and FeCrAl show negligible oxide thickness growth under the current calculation conditions.

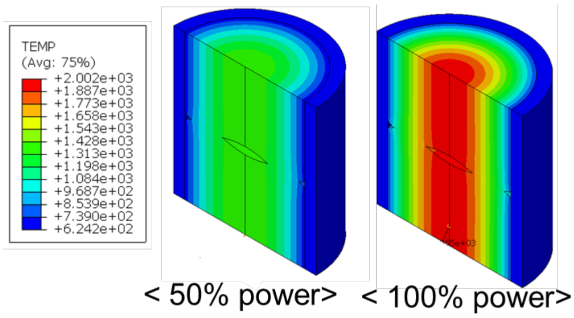

Fig. 3. Beginning-of-life (BOL) Temperature calculation result

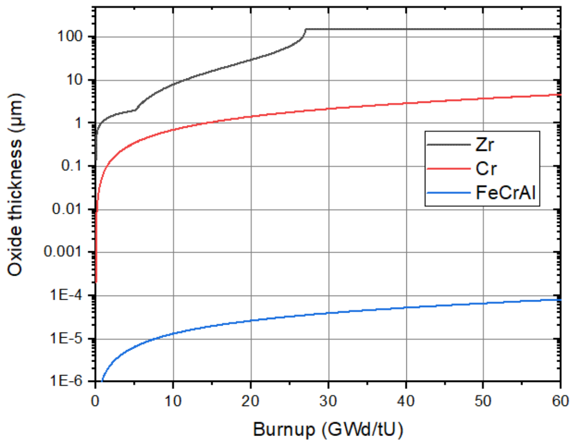

Fig. 4. Oxide thickness calculation result

3. Conclusion

In this study, the effect of coating material and oxidation model on the fuel performance of ATF fuel rod in load following operation was carried out through the developed FEA platform through previous studies. The oxide calculation model was added to the developed platform and used in this study. This result is applied not only to calculations about normal operational scenarios, as demonstrated in the current study, but also to transient events such as Loss of Coolant Accidents (LOCA). It is anticipated that coatings made of chromium (Cr) or iron-chromium-aluminum (FeCrAl) will offer sufficient margin to inhibit phenomena like ballooning or burst under such conditions by preventing severe oxidation. This enhancement in cladding oxidation performance implies the significance of selecting appropriate cladding and coating materials to ensure the structural integrity of fuel rods.

ACKNOWLEDGMENT

This work was supported by the National Research Foundation of Korea (NRF, No. 2022M2E9A304619011) grant funded by the Korea government (MSIT)

REFERENCES

[1] J.C. Brachet, S. Urvoy, E. Rouesne, G. Nony, M. Dumerval, M. Le Saux, F. Ott, A. Michau, F. Schuster, F. Maury, DLI-MOCVD CrxCy coating to prevent Zr-based cladding from inner oxidation and secondary hydriding upon LOCA conditions, J. Nucl. Mater. 550 (2021) 152953. https://doi.org/10.1016/j.jnucmat.2021.152953.

[2] OECD/NEA, Technical and Economic Aspects of Load Following with Nuclear Power Plants, 2011.

[3] J. Mun, H.-J. Kim, H.J. Ryu, Fuel Performance Analysis of Accident-Tolerant Fuel (ATF) Rod with Multi-Layered Cladding During Load Follow Operations, in: Trans. Korean Nucl. Soc. Spring Meet., 2023.

[4] W.G. Luscher, K.J. Geelhood, I.E. Porter, Material Property Correlations :, (2015).

[5] L.J. Siefken, E.W.. . Coryel, E.A. Harvego, J.K. Hohorst, SCDAP/RELAP5/MOD 3.3 Code Manual, 4 (2001) 223.

[6] F. Garzarolli, D. Jorde, R. Manzel, Review of PWR Fuel Rod Waterside Corrosion Behavior, (1980).

[7] B.A. Pint, K.A. Terrani, Y. Yamamoto, L.L. Snead, Material Selection for Accident Tolerant Fuel Cladding, Metall. Mater. Trans. E. 2 (2015) 190–196. https://doi.org/10.1007/s40553-015-0056-7.

[8] B. Jo¨nsson, Q. Lu, D. Chandrasekaran, R. Berglund, F. Rave, Oxidation and Creep Limited Lifetime of Kanthal APMT Ò , a Dispersion Strengthened FeCrAlMo Alloy Designed for Strength and Oxidation Resistance at High, (2013) 29–39. https://doi.org/10.1007/s11085-012-9324-4.

[9] M. Wagih, B. Spencer, J. Hales, K. Shirvan, Fuel performance of chromium-coated zirconium alloy and silicon carbide accident tolerant fuel claddings, Ann. Nucl. Energy. 120 (2018) 304–318. https://doi.org/10.1016/j.anucene.2018.06.001.